2,7-Disubstituted Amidofluorenone Derivatives as Inhibitors of Human Telomerase

Philip J. Perry,[†,§] Martin A. Read,[†] Rhian T. Davies,[†] Sharon M. Gowan,[‡] Anthony P. Reszka,[†] Alexis A. Wood,[†] Lloyd R. Kelland,[‡] and Stephen Neidle*[,†]

Cancer Research Campaign Biomolecular Structure Unit and Centre for Cancer Therapeutics, The Institute of Cancer Research, 15 Cotswold Road, Sutton, Surrey SM2 5NG, U.K.

Received February 19, 1999

Telomerase is a major new target for the rational design of novel anticancer agents. We have previously identified anthraquinone-based molecules capable of inhibiting telomerase by stabilizing G-quadruplex structures formed by the folding of telomeric DNA. In the present study we describe the synthesis and biological evaluation of a series of analogous fluorenone-based compounds with the specific aims of, first, determining if the anthraquinone chromophore is a prerequisite for activity and, second, whether the conventional cytotoxicity inherent to anthraquinone-based molecules may be reduced by rational design. This fluorenone series of compounds exhibits a broad range of telomerase inhibitory activity, with the most potent inhibitors displaying levels of activity (8−12 μM) comparable with other classes of G-quadruplex-interactive agents. Comparisons with analogous anthraquinone-based compounds reveal a general reduction in the level of cellular cytotoxicity. Molecular modeling techniques have been used to compare the interaction of fluorenone- and analogous anthraquinone-based inhibitors with a human G-quadruplex structure and to rationalize their observed biological activities.

Introduction

The telomerase enzyme is a reverse transcriptase which elongates the 3′ ends of telomeric DNA.[1,2] It is not activated in normal somatic cells, which progressively lose telomeric repeats during successive rounds of cell division leading to the nonreplicating state of senescence and ultimately to cell crisis. In contrast, some 80−90% of tumor cells have activated levels of telomerase resulting in stabilization of telomere length and the ability for sustained cellular proliferation.[3] Telomerase is thus an essential factor in cellular immortalization and consequent tumorigenesis.[4] There is currently much interest in the inhibition of telomerase as a novel anticancer strategy.[5] Recent studies have demonstrated inhibition of telomerase activity by antisense oligonucleotides[6] or small-molecule inhibitors,[7] which in turn can result in the onset of senescence and antitumor activity. In order for telomerase inhibitors to be effective as anticancer agents, they may well require long-term administration in order for effective attrition of telomere length to occur after ca. 20 rounds of cell division have taken place. Thus, such agents must have low toxicity toward normal human cells.[8]

Several classes of planar aromatic compounds have been shown to act as telomerase inhibitors.[9] We have recently shown[10] that inhibition of telomerase can be achieved with appropriately substituted diamidoanthraquinone derivatives (**1**) (Figure 1). This inhibition is believed to occur as a result of the stabilization of telomeric DNA by these compounds as folded guanine-quadruplex structures, which are known to inhibit
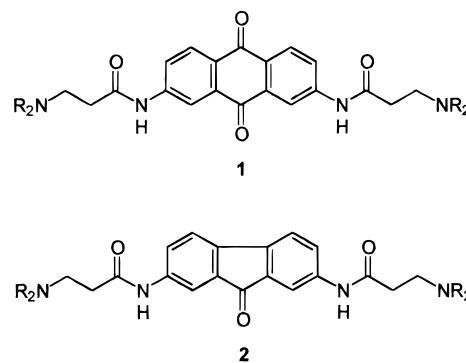

Figure 1. Structures of 2,7-disubstituted anthraquinones **1** and 2,7-disubstituted fluorenones **2** examined in this study.

telomerase activity.[11−14] We have systematically investigated the nature of the terminal amino substituents, the alkyl side-chain linker length,[10a] and the effect of regioisomerism[10b] on telomerase activity for these anthraquinone-based inhibitors. Generally, simple alkylamino, piperidine, and piperazine derivatives attached via propionamido substituents gave optimal activity ([tel]IC$_{50}$ values in the 1−10 μM range) with regioisomer variation showing little effect. Conventional cytotoxicities against a panel of human ovarian tumor cell lines were at levels broadly comparable to telomerase activity. We now report studies on the nature of the chromophore itself to determine, first, if the anthraquinone chromophore is essential for telomerase inhibitory activity and, second, if a component of conventional cytotoxicity (i.e., redox cycling) inherent to quinone-based molecules could be moderated by rational design. This paper describes a series of analogous 2,7-disubstituted fluorenone derivatives (**2**) (Figure 1) in which the central quinone ring has been replaced by a five-membered ring with just one carbonyl substituent.

* Correspondence to: Prof. Stephen Neidle. Tel/fax: +44 181 643 1675. E-mail: steve@iris5.icr.ac.uk.
† CRC Biomolecular Structure Unit.
‡ CRC Centre for Cancer Therapeutics.
§ Present address: School of Pharmacy and Pharmaceutical Sciences, De Montfort University, The Gateway, Leicester LE1 9BH, U.K.

Scheme 1. Synthesis of 2,7-Diamidofluorenone Compounds[a]
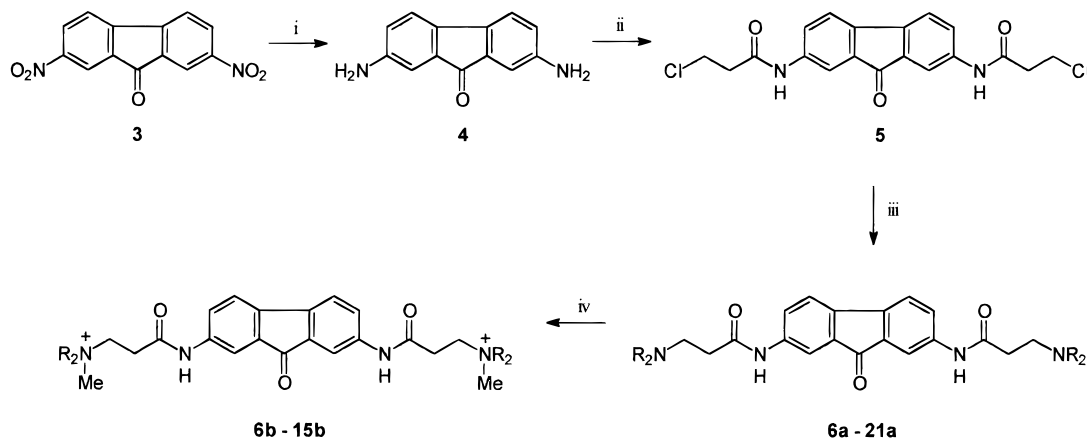
[a] Reagents: (i) $Na_2S \cdot 9H_2O$/NaOH/EtOH/reflux/6 h; (ii) $ClCH_2CH_2COCl$/reflux/4 h; (iii) R_2NH/NaI/EtOH/reflux; (iv) excess MeI/CH_2Cl_2/24 h.

Table 1. Chemical and Physical Properties of the 2,7-Disubstituted Fluorenone Derivatives **6a–21a**

compd	substituent (NR_2)	reaction time (h)	yield (%)	mp (°C)[a]	formula	anal.[b]
6a	NMe_2	8	88	245 (191–192)	$C_{23}H_{28}N_4O_3$	C, H, N
7a	NEt_2	4	84	151 (136–137)	$C_{27}H_{36}N_4O_3 \cdot 0.3H_2O$	C, H, N
8a	4-morpholinyl	18	90	249 (185–186)	$C_{27}H_{32}N_4O_5$	C, H, N
9a	1-piperidinyl	3	86	245–246 (216)	$C_{29}H_{36}N_4O_3 \cdot 0.5H_2O$	C, H, N
10a	1-(2-methyl)piperidinyl	7	84	196–198 (103–105)	$C_{31}H_{40}N_4O_3 \cdot 1.0H_2O$	C, H, N
11a	1-(4-methyl)piperidinyl	22	83	179–180 (207–209)	$C_{31}H_{40}N_4O_3 \cdot 0.5H_2O$	C, H, N
12a	1-(2-ethyl)piperidinyl	20	73	180–182 (61–63)	$C_{33}H_{44}N_4O_3 \cdot 0.5H_2O$	C, H, N
13a	1-(2-hydroxymethyl)piperidinyl	24	77	171–173 (66–68)	$C_{31}H_{40}N_4O_5 \cdot 0.3H_2O$	C, H, N
14a	1-(2-hydroxyethyl)piperidinyl	48	60	163–164 (62–64)	$C_{33}H_{44}N_4O_5 \cdot 0.5H_2O$	C, H, N
15a	1-(4-hydroxy)piperidinyl	72	43	230–232 (184–185)	$C_{29}H_{36}N_4O_5 \cdot 1.0H_2O$	C, H, N
16a	1-(4-methyl)piperazinyl	24	84	255–256 (218–220)	$C_{29}H_{38}N_6O_3 \cdot 0.4H_2O$	C, H, N
17a	1-(4-ethyl)piperazinyl	20	78	247–248 (>300)	$C_{31}H_{42}N_6O_3 \cdot 0.5H_2O$	C, H, N
18a	1-(4-phenyl)piperazinyl	24	52	264–265 (260 dec)	$C_{39}H_{42}N_6O_3 \cdot 0.25H_2O$	C, H, N
19a	1-(4-benzyl)piperazinyl	24	55	207 (240 dec)	$C_{41}H_{46}N_6O_3 \cdot 0.25H_2O$	C, H, N
20a	1-[4-(2-pyridyl)]piperazinyl	72	67	258–259 (204–206)	$C_{37}H_{40}N_8O_3$	C, H, N
21a	1-[4-(2-pyrimidyl)]piperazinyl	72	54	281–283 (102 dec)	$C_{35}H_{38}N_{10}O_3 \cdot 0.25H_2O$	C, H, N

[a] Mp of acid addition salts given in parentheses. [b] Indicated elemental analyses were within ±0.4% of theoretical values.

We have previously reported[10b] on the use of molecular modeling to study diamidoanthraquinone interactions with the folded structure formed by the four-repeat sequence $d[AG_3(T_2AG_3)_3]$ of the human telomere.[15] Ligands were docked into the intercalation site at the 5′-AG step, in accord with NMR data based upon other ligands binding to this sequence.[9b,c] The present study employs an automated docking procedure to locate low-energy positions for fluorenones in this G-quadruplex structure, which we have compared with the corresponding anthraquinone-quadruplex complex.

Chemistry

Synthesis of the bis(aminopropionamido)fluorenones **6a–21a** was accomplished as described in Scheme 1. Briefly, Zinin reduction of 2,7-dinitrofluorenone (**3**) followed by acylation afforded the intermediate chloropropionamide **5** in good yield. Subsequent aminolysis by reflux treatment with the appropriate secondary amine gave the fluorenones **6a–21a** as indicated in Table 1. In addition, quaternary dimethiodide salts of the bis(amino) derivatives **6b–15b** were prepared by treatment with iodomethane.

Results

Telomerase and cytotoxic activity for the 2,7-disubstituted fluorenones **6a–21a** and **6b–15b** are given in Table 2 and are compared with data for the corresponding 2,7-disubstituted anthraquinone derivatives where available. The fluorenone derivatives examined show a broad range of telomerase inhibitory activity with the most potent inhibitor having a [tel]IC$_{50}$ value of 8 μM. Some DNA polymerase selectivity is also suggested, with no inhibition of *Taq* DNA polymerase being observed at equivalent concentrations. The acid addition salts (**6a–12a**) were consistently more active and generally less cytotoxic than the corresponding quaternary dimethiodide derivatives (**6b–12b**). Compound **8a**, containing a morpholine substituent, was found to be totally inactive at concentrations up to 50 μM and follows a trend previously observed for anthraquinone-based molecules.[10] In addition, compounds bearing extended substituents containing an aryl moiety (**18a–21a**) were also found to be inactive. Direct comparisons for compounds **6–9** with analogous 2,7-disubstituted anthraquinone derivatives reveal slightly reduced levels of telomerase inhibition with a similar reduction in cytotoxicity also being evident.

The molecular modeling studies found a single low-energy position (with a total potential energy of −2210 kcal mol^{-1}) for the 2,7-disubstituted diamidoanthraquinone bound to the G-quadruplex complex (Figure 2d). In contrast, two low-energy positional orientations were possible for the analogous fluorenone derivative **9a**, related by approximately 180° of rotation around the molecular long axis. The first of these orientations

Table 2. Telomerase, Cytotoxicity, and *Taq* Polymerase Inhibition Data for Fluorenones **6**−**21**

compd[a]	telIC$_{50}$ (μM)[b]	IC$_{50}$ (μM)[c]			*Taq* inhibition[d]		
		A2780	CH1	SKOV-3	10 μM	20 μM	50 μM
6a	16.2 (4.7)	12 (2.1)	8.5 (4.4)	8.2 (4.15)	−	−	−
6b	18.5 (14.5)	2.25 (0.44)	1.95 (1.3)	1.95 (4)	−	−	−
7a	15.5 (4.3)	14 (2.15)	8 (4.6)	9.65 (7.2)	−	−	−
7b	25.4 (>20)	3.7 (0.33)	2.45 (1.13)	2.4 (2)	−	−	−
8a	≫50 (≫50)	>25 (5.3)	>25 (7.5)	>25 (>100)	−	−	−
8b	27.3 (16.5)	2.55 (0.52)	2.15 (1.1)	2.45 (2.95)	−	−	−
9a	9 (3.1)	11 (0.48)	7.6 (3.15)	11 (3.7)	−	−	−
9b	21 (7.8)	4.3 (0.18)	5.2 (1.05)	3.9 (2.2)	−	−	−
10a	12	10.5	1.8	12	−	−	−
10b	>20	4.85	2.6	3.95	−	−	+
11a	>20	2.2	>25	7.6	−	−	−
11b	>20	2.5	>25	3.75	−	−	+
12a	14	2.2	2.15	3.15	−	−	−
12b	>20	2.9	2.35	2.6	−	−	+
13a	8	13	14	15	−	−	−
13b	33	3.75	4.2	4.3	−	−	−
14a	16.5	>25	14.5	20	−	−	−
14b	>20	5.2	3.15	5.2	−	−	++
15a	18.5	>25	>25	>25	−	−	−
15b	>20	2.4	1.95	4.7	−	−	+
16a	44	>25	>25	>25	−	−	−
17a	17	>25	>25	>25	−	−	−
18a	≫50	>25	>25	>25	−	−	−
19a	≫50	>25	>25	>25	−	−	−
20a	≫50	>25	>25	>25	−	−	−
21a	≫50	>25	>25	>25	−	−	−

[a] Where available, data for the corresponding 2,7-disubstituted anthraquinone derivatives are given in parentheses as published elsewhere.[10b] [b] Concentration required to inhibit telomerase activity by 50% relative to controls. [c] Concentration required to inhibit cell growth by 50% relative to controls. [d] Key: (+++) total, (++) significant, (+) slight, or (−) no inhibition.

(Figure 2a,b) is closely related to that of the corresponding anthraquinone (Figure 2d) and has a potential energy of −2168 kcal mol^{-1}. The second orientation (Figure 2c) has a potential energy of −2163 kcal mol^{-1}. The higher energies of the two fluorenone−G-quadruplex complexes, by 42−47 kcal mol^{-1}, are not due to differences in stacking or other nonbonded energies. Indeed, the intermolecular energy of the fluorenone complex in the first orientation (Figure 2b) is slightly more favorable than that of the anthraquinone complex, due to improved chromophore−base overlap. The observed differences in energies have their origin in the necessity for the fluorenones to induce a measure of distortion in nucleotide backbone conformation at the binding site in order to fit adequately. Thus these differences in potential energy are almost entirely due to increased torsion angle strain energies in the two fluorenone complexes. This also correlates with an observed 3-fold reduction in telomerase activity for the fluorenone compared to the analogous anthraquinone derivative.

Discussion

This study has shown that other tricyclic systems in addition to anthraquinone-based molecules can inhibit telomerase activity. Furthermore, we have demonstrated that conventional cytotoxicity may be moderated through rational design without the loss of telomerase activity. The most potent compounds described here (telIC$_{50}$ values of 8−12 μM) show levels of telomerase inhibitory activity that compare favorably with other classes of G-quadruplex-interactive agents.[9,10] Where direct comparisons with analogous 2,7-disubstituted anthraquinone derivatives are possible (compounds **6**−**9**), the slightly reduced levels of activity shown by the fluorenone derivatives is at first sight surprising

given their structural similarities. However, the change from a six-membered to a five-membered central ring has a significant effect on the shape of the chromophore rendering it crescent-shaped. This, in turn, affects the angular disposition of the aminopropionamido substituents compared to the 2,7-disubstituted anthraquinones, so that a fit of the disubstituted fluorenones into the putative binding site can only be achieved with a degree of distortion of the site and a resultant energy cost. This change also reduces the electron deficiency of the chromophore, so weakening the strength of π-stacking interactions and thus contributing to the reduced affinity of the fluorenone analogue for the G-quadruplex structure. The correlation of lowered activity with the computed reduced potential energy (and, by implication, reduced affinity) for the telomere binding site is further evidence that telomerase inhibition by bis(amido)-substituted tricyclic aromatic molecules proceeds via interaction with and stabilization of folded telomeric DNA. Furthermore, the ability of the molecular modeling to explain the reduced telomerase activity of the fluorenones is yet more evidence in favor of the structural model outlined here.

The results presented here on the fluorenone series of telomerase inhibitors also highlight the need to discover new inhibitors with superior potency against telomerase coupled with lower levels of acute cytotoxicity, to achieve high therapeutic indices. The exploitation of rationally derived structure−activity relationships, such as have been found in this study, is likely to be the key to future success.

Experimental Section

Synthetic Chemistry. Melting points (mp) were recorded on a Leica Galen III hot-stage melting point apparatus and are uncorrected. NMR spectra were recorded at 250 MHz on
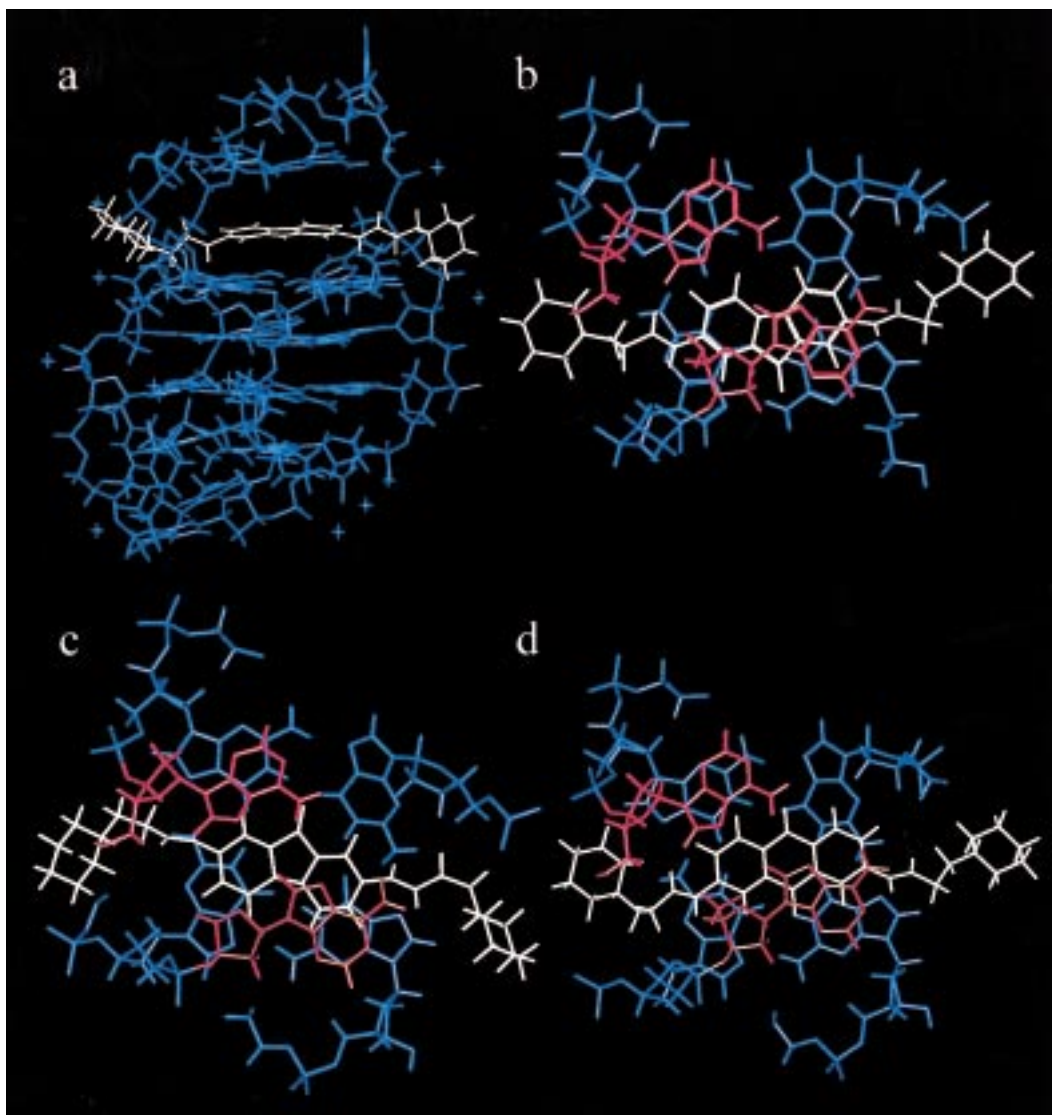
Figure 2. Comparison of binding orientations for the analogous 2,7-disubstituted fluorenone **9a** and anthraquinone derivatives: (a) view of the fluorenone ligand interacting at the 5′-AG step region of the human telomeric G-quadruplex structure; (b) orientation of the fluorenone ligand viewed perpendicular to the plane of the adjacent G-quartet; (c) second orientation of the fluorenone ligand, rotated by approximately 180° around the molecular long axis, and similarly viewed perpendicular to the plane of the adjacent G-quartet; (d) comparative view of the analogous 2,7-disubstituted anthraquinone.

a Bruker AC250 spectrometer in either Me$_2$SO-d_6 or CDCl$_3$ solution at 303 ± 1 K using Me$_4$Si as internal standard. J values are given in hertz (Hz). EI (70 eV), FAB, and high-resolution accurate mass spectra were determined by The School of Pharmacy (University of London, U.K.). Elemental analyses were carried out by Medac Ltd. (Brunel Science Center, Egham, Surrey, U.K.); results for elements indicated by symbols were within ±0.4% of theoretical values. TLC was carried out on silica gel (Merck 60F-254) using CHCl$_3$−MeOH (0−20% MeOH) as eluent, with visualization at 254 and 366 nm. Organic solutions were dried over sodium sulfate. Acid addition salts were prepared by standard literature methods. The 2,7-disubstituted anthraquinone derivative described in this study was prepared as described previously.[10b]

2,7-Diamino-9-fluorenone (4). To a stirred suspension of 2,7-dinitro-9-fluorenone (**3**) (9.45 g, 35 mmol) in ethanol (375 mL) was added a solution of sodium sulfide nonahydrate (37.85 g, 157.5 mmol) and sodium hydroxide (15 g, 375 mmol) in water (650 mL). The mixture was heated at reflux for 5 h and left to stand overnight. The mixture was cooled to 0−5 °C and the resulting precipitate collected by filtration. The crude product was washed successively with water (2 × 100 mL), aqueous NaOH (2 × 100 mL, 5% w/v), water (3 × 100 mL), cold EtOH (2 × 50 mL), ether (50 mL), and hexane (50 mL)

and dried in vacuo. Recrystallization from acetone−ethanol (1:1 v/v) afforded the fluorenone **4** (6.30 g, 86%) as purple needles: mp 278−279 °C; NMR δ (DMSO) 5.32 (4H, br s, NH$_2$) 6.57 (2H, dd, J = 7.9, 2.1, H-3,6), 6.69 (2H, d, J = 2.1, H-1,8), 7.09 (2H, d, J = 7.9, H-4,5); MS (rel intensity) m/z 210 (100); calcd ([M + 1]$^+$) 210.0793, found 210.0780. Anal. (C$_{13}$H$_{10}$N$_2$O) C, H, N.

2,7-Bis(3-chloropropionamido)-9-fluorenone (5). A stirred suspension of 2,7-diamino-9-fluorenone (**4**) (6.3 g, 30 mmol) and 3-chloropropanoyl chloride (50 mL, 0.525 mol) in xylene (200 mL) was heated at reflux for 1.5 h and cooled to 0−5 °C. The crude product was collected by filtration, washed with toluene (2 × 100 mL), acetone (100 mL), EtOH (100 mL), and ether (100 mL), and dried in vacuo. Recrystallization from DMF−EtOH (2:1 v/v) afforded chloroamide **5** (9.39 g, 80%) as salmon-pink crystals: mp 328 °C dec; NMR δ (DMSO) 2.85 (4H, t, J = 6.1, COCH$_2$), 3.90 (4H, t, J = 6.1, CH$_2$Cl), 7.62 (2H, t, J = 8.1, H-4,5), 7.70 (2H, dd, J = 8.1, 1.9, H-3,6), 7.92 (2H, d, J = 1.9, H-1,8), 10.31 (2H, s, NH); MS (rel intensity) m/z 391 (100), 373 (46), 355 (72), 301 (76), 289 (84), 231 (96), 210 (91); calcd ([M + 1]$^+$) 391.0616, found 391.0610. Anal. (C$_{19}$H$_{16}$N$_2$O$_3$Cl$_2$·0.1H$_2$O) C, H, N.

2,7-Bis[3-(dimethylamino)propionamido]-9-fluorenone (6a). General Aminolysis Procedure. Dimethylamine

(5.4 mL of 33% w/w solution in EtOH, 30 mmol) was added during 15 min to a stirred, refluxing suspension of chloroamide **5** (0.936 g, 2.4 mmol) and NaI (0.25 g) in EtOH (50 mL). After refluxing for the indicated time period (see Table 1), the mixture was cooled to 0−5 °C and KOH pellets (5 g) were added. The mixture was stirred for 1 h, and the resulting precipitate was collected by filtration, washed with ether (50 mL), and dried in vacuo. The crude product was dissolved in CHCl$_3$ (100 mL), washed with water (2 × 50 mL), and dried. Evaporation and recrystallization from EtOH gave the amide **6a** (0.86 g, 88%) as an orange solid: mp 245 °C; NMR δ (CDCl$_3$) 2.39 (12H, s, CH$_3$), 2.52 (4H, m, CH$_2$N), 2.64 (4H, m, COCH$_2$), 7.38 (2H, d, $J = 8.1$, H-4,5), 7.47 (2H, d, $J = 1.9$, H-1,8), 7.96 (2H, dd, $J = 8.1, 1.9$, H-3,6), 11.21 (2H, s, NH); MS (rel intensity) m/z 409 (100); calcd ([M + 1]$^+$) 409.2240, found 409.2211. Anal. (C$_{23}$H$_{28}$N$_4$O$_3$) C, H, N. Maleate salt: mp 191−192 °C.

2,7-Bis[3-(dimethylamino)propionamido]-9-fluorenone N,N-Dimethiodide (6b). General Procedure. To a solution of **6a** (0.408 g, 1 mmol) in dichloromethane (50 mL) was added iodomethane (3.3 mL, 50 mmol), and the solution stirred at room temperature for 24 h. The resulting precipitate was collected by filtration, washed with dry ether, and dried in vacuo at 25 °C to give dimethiodide **6b** (0.67 g, 97%) as an orange solid: mp 234−235 °C; NMR δ (DMSO) 2.92 (4H, t, $J = 7.5$, COCH$_2$), 3.10 (18H, s, N$^+$CH$_3$), 3.67 (4H, t, $J = 7.5$, CH_2N$^+$), 7.65 (4H, br m, ArH), 7.91 (2H, br s, ArH), 10.39 (2H, br s, NH). Anal. (C$_{25}$H$_{34}$N$_4$O$_3$I$_2$·2H$_2$O) C, H, N, I.

***Taq* Polymerase Assay.** Compounds were tested as their acid addition (**6a−15a** as hydrochlorides, **16a−21a** as maleates) and quaternary dimethiodide (**6b−15b**) salts at 10, 20, and 50 μM final concentrations in a PCR 50-μL master mix containing 10 ng of pCI-neo mammalian expression vector (Promega, Southampton, U.K.) and forward (GGAGTTC-CGCGTTACATAAC) and reverse (GTCTGCTCGAAGCAT-TAACC) primers (200 nmol) as described previously.[10a] The product of approximately 1 kb was visualized on a 2% w/w agarose gel following amplification (30 cycles of 94 °C for 1 min, 55 °C for 1 min, and 72 °C for 2.5 min).

Modified Telomeric Repeat Amplification Protocol (TRAP) Assay. The ability of agents to inhibit telomerase in a cell-free assay was assessed with a modified TRAP assay using extracts from exponentially growing A2780 human ovarian carcinoma cells as described previously.[10a] The TRAP assay was performed in two steps: (a) telomerase-mediated extension of the forward primer (TS: 5′-AATCCGTCGAGCA-GAGTT; Oswel Ltd., Southampton, U.K.) contained in a 40-μL reaction mix comprising TRAP buffer (20 mM Tris-HCl (pH 8.3), 68 mM KCl, 1.5 mM MgCl$_2$, 1 mM EGTA, 0.05% v/v Tween 20), 0.05 μg of bovine serum albumin, 50 μM of each deoxynucleotide triphosphate, 0.1 μg of TS primer, and 3 μCi of [α-^{32}P]dCTP (Amersham plc, U.K.). Protein (0.04 μg) was then incubated with the reaction mix ± agent (acid addition and quaternary dimethiodide salts) at final concentrations of up to 50 μM for 20 min at 25 °C. A lysis buffer (no protein) control, heat-inactivated protein control, and 50% protein (0.02 μg) control were included in each assay. (b) While heating at 80 °C in a PCR block of a thermal cycler (Hybaid, U.K.) for 5 min to inactivate telomerase activity, 0.1 μg of reverse CX primer (3′-AATCCCATTCCCATTCCCATTCCC-5′) and 2 units of *Taq* DNA polymerase ("red hot", Advanced Biotechnologies) were added. A three-step PCR was then performed: 94 °C for 30 s, 50 °C for 30 s, and 72 °C for 1 min for 31 cycles. Telomerase-extended PCR products in the presence or absence of compounds were then determined either by electrophoretic separation using 8% w/w acrylamide denaturing gels and analysis by phosphorimaging or autoradiography or by harvesting on Whatman filters (25-mm glass microfiber) and analysis by liquid scintillation counting.

Growth Inhibition Assay. Growth inhibition was measured in three human ovarian carcinoma cell lines (A2780, CH1, and SKOV-3) using the sulforhodamine B (SRB) assay as described previously.[16] Briefly, between 3000 and 6000 cells were seeded into the wells of 96-well microtiter plates and allowed to attach overnight. Agents (acid addition and quaternary dimethiodide salts) were dissolved at 500 μM in water and immediately added to wells in quadruplicate at final concentrations of 0.05, 0.25, 1, 5, and 25 μM. Following an incubation period of 96 h, remaining cells were fixed with ice-cold 10% w/v trichloroacetic acid (30 min) and stained with 0.4% SRB in 1% v/v acetic acid (15 min). Mean absorbance at 540 nm for each drug concentration was expressed as a percentage of the control untreated well absorbance, and IC$_{50}$ values (concentration required to inhibit cell growth by 50%) were determined for each agent.

Molecular Modeling Studies. The Macromodel 5.0 program[17] using the AMBER* force field with continuum solvation treatment (GB/SA model of water solvation, van der Waals cutoff 8 Å, electrostatic cutoff 20 Å, dielectric constant 1) was employed for initial model building and calculations. Coordinates from the solution NMR structure of the human telomeric repeat d[AG$_3$(T$_2$AG$_3$)$_3$] G-quadruplex[15] were used to give an initial low-energy starting model. Molecular mechanics energy minimization (1000 steps steepest descent with line searching and 3000 steps Polak Ribiere conjugate gradient with derivative convergence of 0.05 kJ/Å mol) followed by dynamics (1.5-fs time step, 40 ps at 300 K equilibrium, 100 ps at 300 K production with time averaging of 100 sampled structures) and subsequent mechanics (minimization of time-averaged dynamics structure) was used. An intercalation site was introduced between the diagonal T$_2$A loop and the G-quartet segment of the structure (the 5′-AG step) by breaking the phosphate backbones and separating the structure while monitoring the distance between the segments. The sugar−phosphate chains were reconnected, and molecular mechanics energy minimization (1000 steps steepest descent with line searching followed by 1000 steps conjugate gradient) was used to relieve any resulting steric distortion while retaining the G-quartet and loop motifs with positional restraints.

Models for the fluorenone and anthraquinone molecules with 2,7-bis(3-piperidinopropionamido) substituents were created, minimized, and docked into the intercalation site using the DOCKING module within the INSIGHTII package.[18] This enables molecular orientation to be explored while monitoring electrostatic and van der Waals ligand and DNA interactions. Both ligand and intercalation site geometries were allowed to vary during the search. Possible starting orientations were chosen by means of a Monte Carlo algorithm. Individual bases were constrained at this initial docking stage, although the backbone around the intercalation site was unconstrained. The best chromophore positions were subjected to 100 steps of unconstrained molecular mechanics minimization. The final ranking order of structures was based on the resulting energy values.

References

(1) (a) Blackburn, E. H. Structure and Function of Telomeres. *Nature* **1991**, *350*, 569−573. (b) Kipling, D. Mammalian Telomerase: Catalytic Subunit and Knockout Mice. *Human Mol. Genet.* **1997**, *6*, 1999−2004.

(2) (a) Harley, C. B.; Futcher, A. B.; Greider, C. W. Telomeres Shorten During Aging of Human Fibroblasts. *Nature* **1990**, *345*, 458−460. (b) Allsopp, R. C.; Harley, C. B. Evidence for a Critical Telomere Length in Senescent Human Fibroblasts. *Exp. Cell Res.* **1995**, *219*, 130−136.

(3) (a) Kim, N. W.; Piatyszek, M. A.; Prowse, K. R.; Harley, C. B.; West, M. D.; Ho, P. L. C.; Coviello, G. M.; Wright, W. E.; Weinrich, R. L.; Shay, J. W. Specific Association of Human Telomerase Activity with Immortal Cells and Cancer. *Science* **1994**, *266*, 2011−2015. (b) Counter, C. M.; Hirte, H. W.; Bacchetti, S.; Harley, C. B. Telomerase Activity in Human Ovarian Carcinoma. *Proc. Natl. Acad. Sci. U.S.A.* **1994**, *91*, 2900−2904. (c) Tang, R.; Cheng, A.-J.; Wang, J.-Y.; Wang, T.-C. V. Close Correlation between Telomerase Expression and Adenomatous Polyp Progression in Multistep Colorectal Carcinogenesis. *Cancer Res.* **1998**, *58*, 4052−4054. (d) Hoos, A.; Hepp, H. H.; Kaul, S.; Ahlert, T.; Bastert, G.; Wallwiener, D.

Telomerase Activity Correlates with Tumor Aggressiveness and Reflects Therapy Effect in Breast Cancer. *Int. J. Cancer* **1998**, *79*, 8−12. (e) Sano, T.; Asai, A.; Fujimaki, T.; Kirino, T. Telomerase Activity in 144 Brain Tumours. *Br. J. Cancer* **1998**, *77*, 1633−1637.

(4) (a) Bodnar, A. G.; Ouellette, M.; Frolkis, M.; Holt, S. E.; Chiu, C. P.; Morin, G. B.; Harley, C. B.; Shay, J. W.; Lichtsteiner, S.; Wright, W. E. Extension of Life-span by Introduction of Telomerase into Normal Human Cells. *Science* **1998**, *279*, 349−352. (b) Niida, H.; Matsumoto, T.; Satoh, H.; Shiwa, M.; Tokutake, Y.; Furuichi, Y.; Shinkai, Y. Severe Growth Defect in Mouse Cells Lacking the Telomerase RNA Component. *Nature Genet.* **1998**, *19*, 203−206. (c) Blasco, M. A.; Lee, H.-W.; Hande, M. P.; Samper, E.; Lansdorp, P. M.; DePinho, R. A.; Greider, C. W. Telomere Shortening and Tumor Formation by Mouse Cells Lacking Telomerase RNA. *Cell* **1997**, *91*, 25−34. (d) Lee, H.-W.; Blasco, M. A.; Gottlieb, G. J.; Horner, J. W.; Greider, C. W.; DePinho, R. A. Essential Role of Mouse Telomerase in Highly Proliferative Organs. *Nature* **1998**, *392*, 569−574.

(5) (a) Perry, P. J.; Kelland, L. R. Telomeres and Telomerase: Targets for Cancer Chemotherapy. *Exp. Opin. Ther. Patents* **1998**, *8*, 1567−1586. (b) Raymond, E.; Sun, D.; Chen, S.-F.; Windle, B.; von Hoff, D. D. Agents that Target Telomerase and Telomeres. *Curr. Opin. Biotechnol.* **1996**, *7*, 583−591.

(6) (a) Hamilton, S. E.; Pitts, A. E.; Katipally, R. R.; Jia, X.; Rutter, J. P.; Davies, B. A.; Shay, J. W.; Wright, W. E.; Corey, D. R. Identification of Determinants for Inhibitor Binding within the RNA Active Site of Human Telomerase Using PNA Scanning. *Biochemistry* **1997**, *36*, 11873−11880. (b) Kondo, S.; Kondo, Y.; Li, G.; Silverman, R. H.; Cowell, J. K. Targeted Therapy of Human Malignant Glioma in a Mouse Model by 2-5A Antisense Directed Against Telomerase RNA. *Oncogene* **1998**, *16*, 3323−3330. (c) Bisoffi, M.; Chakerian, A. E.; Fore, M. L.; Bryant, J. E.; Hernandez, J. P.; Moyzis, R. K.; Griffith, J. K. Inhibition of Human Telomerase by a Retrovirus Expressing Telomeric Antisense RNA. *Eur. J. Cancer* **1998**, *34*, 1242−1249. (d) Glukhov, A. I.; Zimnik, O. V.; Gordeev, S. A.; Severin, S. E. Inhibition of Telomerase Activity of Melanoma Cells *in Vitro* by Antisense Oligonucleotides. *Biochem. Biophys. Res. Commun.* **1998**, *248*, 368−371.

(7) (a) Strahl, C.; Blackburn, E. H. Effects of Reverse Transcriptase Inhibitors on Telomere Length and Telomerase Activity in Two Immortalised Human Cell Lines. *Mol. Cell. Biol.* **1996**, *16*, 53−65. (b) Yegorov, Y. E.; Chernov, D. N.; Akimov, S. S.; Bolsheva, N. L.; Krayevsky, A. A.; Zelenin, A. V. Reverse Transcriptase Inhibitors Suppress Telomerase Function and Induce Senescence-like Processes in Cultured Mouse Fibroblasts. *FEBS Lett.* **1996**, *389*, 115−118. (c) Melana, S. M.; Holland, J. F.; Pogo, B. G.-T. Inhibition of Cell Growth and Telomerase Activity of Breast Cancer Cells In Vitro by 3′-Azido-3′-deoxythymidine. *Clin. Cancer Res.* **1944**, *4*, 693−696. (d) Fletcher, T. M.; Salazar, M.; Chen, S.-F. Human Telomerase Inhibition by 7-Deaza-2′-deoxy-purine Nucleoside Triphosphates. *Biochemistry* **1996**, *35*, 15611−15617. (e) Yamakuchi, M.; Nakata, M.; Kawahara, K.-I.; Kitajima, I.; Maruyama, I. New Quinolones, Ofloxacin and Levofloxacin, Inhibit Telomerase Activity in Transitional Cell Carcinoma Cell Lines. *Cancer Lett.* **1997**, *119*, 213−219. (f) Pai, R. B.; Pai, B.; Kukhanova, M.; Dutschman, G. E.; Guo, X.; Cheng, Y.-C. Telomerase from Human Leukemia Cells: Properties and Its Interaction with Deoxynucleoside Analogues. *Cancer Res.* **1998**, *58*, 1909−1913. (g) Gomez, D. E.; Tejera, A. M.; Olivero, O. A. Irreversible Telomere Shortening by 3′-Azido-2′,3′-Dideoxythymidine (AZT) Treatment. *Biochem. Biophys. Res. Commun.* **1998**, *246*, 107−110.

(8) Venitt, S.; Crofton-Sleigh, C.; Agbandje, M.; Jenkins, T. C.; Neidle, S. Anthracene-9,10-diones as Potential Anti-Cancer Agents: Bacterial Mutation Studies of Amido-Substituted Derivatives Reveal an Unexpected Lack of Mutagenicity. *J. Med. Chem.* **1998**, *41*, 3748−3752.

(9) (a) Sun, D.; Thompson, B.; Cathers, B. E.; Salazar, M.; Kerwin, S. M.; Trent, J. O.; Jenkins, T. C.; Neidle, S.; Hurley, L. H. Inhibition of Human Telomerase by a G-Quadruplex-Interactive Compound. *J. Med. Chem.* **1997**, *40*, 2113−2116. (b) Wheelhouse, R.; Sun, D.; Han, H.; Han, F. X.; Hurley, L. H. Cationic Porphyrins as Telomerase Inhibitors: the Interaction of Tetra-(*N*-methyl-4-pyridyl)porphine with Quadruplex DNA. *J. Am. Chem. Soc.* **1998**, *120*, 3261−3262. (c) Federoff, O. V.; Salazar, M.; Han, H.; Chemeris, V. V.; Kerwin, S. M.; Hurley, L. H. NMR-Based Model of a Telomerase-Inhibiting Compound Bound to G-Quadruplex DNA. *Biochemistry* **1998**, *37*, 12367−12374.

(10) (a) Perry, P. J.; Gowan, S. M.; Reszka, A. P.; Polucci, P.; Jenkins, T. C.; Kelland, L. R.; Neidle, S. 1,4- and 2,6-Disubstituted Amidoanthracene-9,10-dione Derivatives as Inhibitors of Human Telomerase. *J. Med. Chem.* **1998**, *41*, 3253−3260. (b) Perry, P. J.; Reszka, A. P.; Wood, A. A.; Read, M. A.; Gowan, S. M.; Dosanjh, H. S.; Trent, J. O.; Jenkins, T. C.; Kelland, L. R.; Neidle, S. Human Telomerase Inhibition by Regioisomeric Disubstituted Amidoanthracene-9,10-diones. *J. Med. Chem.* **1998**, *41*, 4873−4884.

(11) Williamson, J. R. G-quartet Structures in Telomeric DNA. *Annu. Rev. Biophys. Biomol. Struct.* **1994**, *23*, 703−730.

(12) Zahler, A. M.; Williamson, J. R.; Cech, T. R.; Prescott, D. M. Inhibition of Telomerase by G-quartet DNA Structures. *Nature* **1991**, *350*, 718−720.

(13) Fletcher, T. M.; Sun, D.; Salazar, M.; Hurley, L. H. Effect of DNA Secondary Structure on Human Telomerase Activity. *Biochemistry* **1998**, *37*, 5536−5541.

(14) Mergny, J.-L.; Hélène, C. G-Quadruplex DNA: a Target for Drug Design. *Nature Medicine* **1998**, *4*, 1366−1367.

(15) Wang, Y.; Patel, D. J. Solution Structure of the Human Telomeric Repeat d[AG$_3$(T$_2$AG$_3$)$_3$] G-tetraplex. *Structure* **1993**, *1*, 263−282.

(16) Kelland, L. R.; Abel, G.; McKeage, M. J.; Jones, M.; Goddard, P. M.; Valenti, M.; Murrer, B. A.; Harrap, K. R. Preclinical Antitumor Evaluation of Bis-acetato-amine-dichloro-cyclohexylamine Platinum(IV): an Orally Active Platinum Drug. *Cancer Res.* **1993**, *53*, 2581−2586.

(17) Mohamadi, F.; Richards, N. G. J.; Guida, W. C.; Liskamp, R.; Lipton, M.; Caufield, C.; Chang, G.; Hendrickson, T.; Still, W. C. Macromodel − an Integrated Software System for Modeling Organic Bioorganic Molecules using Molecular Mechanics. *J. Comput. Chem.* **1990**, *11*, 440−467.

(18) Luty, B. A.; Wasserman, Z. R.; Stouten, P. F. W.; Hodge, C. N.; Zacharias, M.; McCammon, J. A. A Molecular Mechanics/Grid Method for Evaluation of Ligand−Receptor Interactions. *J. Comput. Chem.* **1995**, *16*, 454−464.